2017 International Conference on Mechanical, System and Control Engineering

Humanoid Robot Kinematic Calibration Using Industrial Manipulator

Ramil Khusainov, Alexandr Klimchik
Laboratory of Intelligent Robotic Systems (LIRS)
Innopolis University
Innopolis, Tatarstan, Russian Federation
e-mail:{r.khusainov, a.klimchik}@innopolis.ru

Evgeni Magid
Higher Institute of Information Technology &
Information Systems
Kazan Federal University
Kazan, Russian Federation
e-mail: magid@it.kfu.ru

***Abstract*—Kinematic calibration is a crucial task for humanoid robot locomotion. The paper proposes a novel technique for joint offset calibration using industrial manipulator. Corresponding procedure uses position and orientation data from the manipulator and requires fixing of robots bases and end-effectors with respect to each other. The full pose information is obtaining as the humanoid limbs are moved through predefined configurations. To find joint offsets the least-squares optimization problem is solved. The proposed method is accurate since the industrial manipulator provides high precision. The proposed approach was validated on the calibration of AR601M humanoid robot using Kuka iiwa 14 industrial manipulator.**

Keywords-humanoid; calibration; AR601M; KUKA iiwa; industrial manipulator

I. Introduction

The majority of modern humanoid control algorithms are based on robot kinematic and dynamic models. Therefore, identification of model parameters is a crucial requirement for effective robot performance such as walking, manipulation and navigation.

Joint offset calibration is one of the most important problems since unlike model kinematic parameters, encoder offsets cannot be extracted directly from CAD model. Especially it becomes important when robot manufacturer does not provide "factory" angle calibration of the robot and "zero" poses in actuators are not defined. Also, as the robot is subjected to experiments with collisions, due to wear or reassembly it should be periodically calibrated. Several self-calibration methods have been developed lately to address this issue [1-6]. Guedelha et al. [3] uses a distributed set of on-board accelerometers and solve unconstrained nonlinear least squares optimization problem based on collected measurements during robot's slow motion. But there were several assumptions such that the relative pose of each accelerometer with respect to its support link is known precisely a priori which cannot be always realized. Also method's accuracy highly depends on inertial sensors' noise level in this case. In [4, 5] authors use stereo cameras of the robot to calculate relative position of the limbs and calibrate robot. Asfour et al. [7] proposed a method to calibrate camera's relative position to the head by observing a marker. For their approach camera intrinsic parameters should be known before experiments. Birbach et al. [4] proposed an approach of calibrating camera parameters, upper body joint elasticities and joint offsets as well as head mounted IMU by solving combined optimization problem for a single point marker positions. However, their approach depends on a given rough initial guess which cannot be always well known a priori. Maier et al. [5] present an approach for kinematic model calibration based on robot's monocular camera. Algorithm automatically chooses robot configurations that enable an optimal calibration procedure. In this case accuracy depends on camera characteristics and initial estimation of marker positions. It has large number of parameters and needs initial joint zero state provided by the manufacturer. Yamane [8] proposed a calibration method for humanoid's legs based on chest-mounted IMU data and the constraint that the feet are fixed on the ground plane while moving the body. However, robot arms cannot be calibrated with such a method. Additionally, IMU sensor should be well calibrated and precise in angle measurement which is not always achieved.

Kinematic parameters calibration problem has been thoroughly studied previously in the context of industrial manipulators calibration [9-13]. Main approaches are based on kinematic constraints [9], on-board measurement sensors [11], partial-pose measurement using laser tracking systems [12], stereo-vision systems [14] and other devices, which usually provide a guaranteed level of accuracy. In [10] authors present an enhanced method of geometric calibration which reduces the measurement noise by means of proper configuration selection and demonstrates good accuracy improvement. The difficulty of applying such methods for floating-base humanoids is the necessity of fixing the robot body. At the same time the benefits of these approach, such as accuracy improvement, ability to calibrate both manipulators and pedipulators as well as sensors and possibility to estimate dynamic parameters by measuring force-torque data are obvious.

In our work we use KUKA LBR iiwa R820 7DoF manipulator robot as the measurement system to calibrate AR601M humanoid robot. Due to its impedance control with zero reaction the manipulator can follow the humanoid's end-effector with no resistance and provides us with 6 DoF accurate position data (position repeatability is ±0.15 mm). And more importantly when humanoid is static it can exert specific external force by the means of its force sensors and simultaneously measure the end-effector position changes. Therefore, it combines functionalities of full pose measurement system with enough accuracy and 6 DoF force\torque sensor. Processing of force-torque data to estimate dynamic parameters of the humanoid robot, such as stiffness matrix, and to calibrate robot's force-torque sensors is ongoing research.

The remainder of the paper is organized as follows. We formulate problem in the next section. Section III describes geometric parameters identification method. Experimental results are given in Section IV and conclusions are made in V.

II. Problem Statement

In robotics calibration is the process of determining robot's geometric parameters. While some parameters like link length can be directly derived from CAD model and their deviations are relatively small, joint encoder offsets are not known a priori and their definition depends on kinematic model and encoder assembly procedure. The robot actual *i*-th joint angle θ_i depends also on the encoder offset Δq_i and can be expressed as $\theta_i = q_i + \Delta q_i$, where q_i is corresponding encoder angle. The simplest way to obtain joint offset Δq_i is to align adjacent links, making $\theta_i = 0$, and get the encoder value. However, achievement of this specific links alignment is not a trivial task and requires external measurement tools. Moreover, this approach can be hardly applied for the links with irregular shape.

Let us consider a humanoid robot shown in Fig. 1. If we fix robot's trunk then each arm and leg can be considered as a serial chain manipulator, whose end-effector (foot or wrist) location $\mathbf{t} = (\mathbf{p}, \boldsymbol{\varphi})$ (position $\mathbf{p}$ and orientation $\boldsymbol{\varphi}$) can be computed using forward kinematics

$$\mathbf{t} = g(\mathbf{q}, \Delta\mathbf{q}, \mathbf{T}_{base}, \mathbf{T}_{tool}) \tag{1}$$

where function g(..) defines geometric model, q is the vector of actuated joint angles from encoders, $\Delta\mathbf{q}$ is the vector of joint offsets, $\mathbf{T}_{base}, \mathbf{T}_{tool}$ are base and tool transformation matrices. If we carry out a set of experiments where the end-effector locations are measured by an external device for several configurations defined by vector $\mathbf{q}_i$, then related optimization problem allowing us to estimate joint offsets can be formulated as follows

$$\sum_{i=1}^{m} \left\| \mathbf{t}_i^0 - g(\mathbf{q}_i, \Delta\mathbf{q}, \mathbf{T}_{base}, \mathbf{T}_{tool}) \right\|^2 \to \min_{\Delta\mathbf{q}} \tag{2}$$

where $\mathbf{t}_i^0$ is a vector of measured end-effector locations for *i*-th configuration*, m is number of measurement configurations*. The main difficulty here is that although $\mathbf{T}_{base}$ and $\mathbf{T}_{tool}$ transformation matrices are the same for each configuration they are initially unknown and cannot be neglected. So, we need first to estimate them approximately and include corresponding errors as additional parameters in the main identification problem. Another difficulty is related to definition of vector norm in (2), where six-dimensional residuals are not homogeneous. To overcome this difficulty, it is proposed to divide search algorithm into sub steps where Cartesian coordinates residuals and angle residuals are used separately.

Hence, the goal of this work is to obtain joint offsets for the humanoid robot AR-601M with precision on the level of encoder error, which is about $0.1°$.

III. Calibration Method

A. Experimental Setup

The considered anthropomorphic robot AR-601M and related kinematic chains of its leg and arm are shown in Fig. 1. Developed calibration procedure uses KUKA LBR iiwa 14 R820 manipulator as a measurement device. The main idea of the experimental setup is shown in Fig. 2, where humanoid trunk is fix with respect to the manipulator base and manipulator end effector is connected to humanoid foot/wrist mechanically. Manipulator can work in zero impedance mode, i.e. it can follow the humanoid end-effector without resistance. Thus, it can provide us with accurate end-effector position and orientation directly from the manipulator for different configurations of humanoid leg with linear accuracy 0.15 mm.

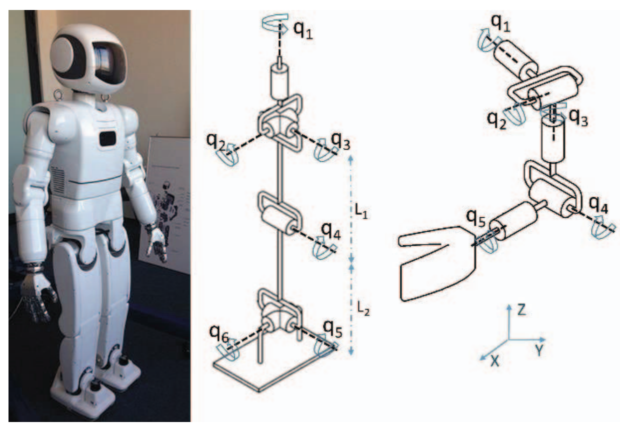

Figure 1. AR601M robot and kinematic models of its leg and arm.

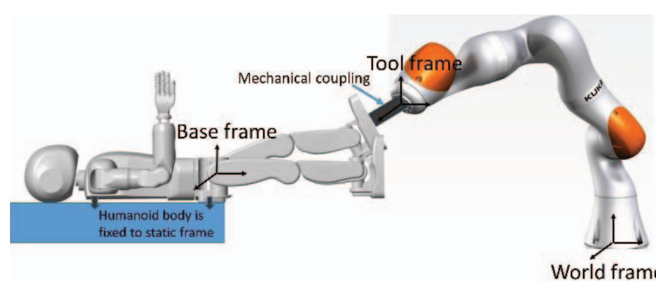

Figure 2. Sketch of the calibration process showing humanoid AR601M leg attached to KUKA manipulator.Maintaining the Integrity of the Specifications

B. Identification Algorithm.

1) World, base, foot and tool frames.

The world frame (F_W) is the reference for end-effector location measurements in experiments and located in KUKA manipulator base. The base frame (F_B) is connected with humanoid body and its origin is located in intersection of three hip joint axes. The foot frame (F_F) is connected with humanoid foot and its origin is located in intersection of humanoid ankle joints. The tool frame (F_T) is located in manipulator's end-effector. KUKA robot's software outputs position and orientation of tool frame relative to world frame. Alternatively, we can calculate tool frame location using humanoid's kinematics.

2) Kinematic model

Let us derive tool frame position using humanoid leg forward kinematics. Given a joint angle vector $\mathbf{q}=\left[q_1 ... q_6\right]^T$ and joint offsets vector $\Delta\mathbf{q}=\left[\Delta q_1 ... \Delta q_6\right]^T$ we can write

$$\mathbf{T}_{world}^{tool}=\mathbf{T}_{base}\mathbf{T}_{robot}(\mathbf{q},\Delta\mathbf{q})\mathbf{T}_{tool} \tag{3}$$

where $\mathbf{T}_{base}$ is transformation matrix from F_W to F_B, $\mathbf{T}_{tool}$ is transformation matrix from F_F to F_T, and the transformation matrix $\mathbf{T}_{robot}$ describes the humanoid leg geometry. From kinematic model shown in Fig.1 we can write

$$\begin{aligned}\mathbf{T}_{robot}&=\mathbf{R}_z(q_1+\Delta q_1)\mathbf{R}_x(q_2+\Delta q_2)\mathbf{R}_y(q_3+\Delta q_3)\mathbf{A}_z(L_1)\\ &\mathbf{R}_y(q_4+\Delta q_4)\mathbf{A}_z(L_2)\mathbf{R}_y(q_5+\Delta q_5)\mathbf{R}_x(q_6+\Delta q_6)\end{aligned} \tag{4}$$

where $\mathbf{R}_x,\mathbf{R}_y,\mathbf{R}_z$ are elementary rotation transformation matrices and $\mathbf{A}_z$ is translation transformation matrix. Notice that (3) has totally 18 unknown parameters: 6 in each $\mathbf{T}_{base}$ and $\mathbf{T}_{tool}$ and 6 in $\Delta\mathbf{q}$ vector.

3) Parameters initialization

Before we continue with parameters search algorithm we need to initialize them. Since joint offsets values are relatively small, we set their initial values as zeros $\Delta\mathbf{q}=0$. Initial base and tool locations are found by rotating corresponding joints. For example, to locate base frame we firstly rotate first joint around z axis. By measuring end effector positions we can identify rotation axis vector. Then we repeat the procedure for second joint. Intersection of two rotation axes will give us base frame origin. Orientation of base frame is calculated from rotation axes directions.

4) Search algorithm

Let us assume that we have measured the Cartesian coordinates $\mathbf{p}^i=(p_x^i,p_y^i,p_z^i)^T$ and orientation angles $\boldsymbol{\varphi}_i=(\varphi_x^i,\varphi_y^i,\varphi_z^i)^T$ for m configurations. To simplify computations it is proposed to split the identification procedure into two steps. The first step deals with base and tool parameters identification $\mathbf{p}_{base},\boldsymbol{\varphi}_{base}$, $\mathbf{p}_{tool},\boldsymbol{\varphi}_{tool}$, assuming that bipedal parameters are known. The second step focuses on estimation of $\Delta\mathbf{q}$ vector under assumption that base and tool parameters are already identified. These two steps are repeated iteratively until converge to desired accuracy.

Step 1. Taking into account that in the experimental study initial estimation of base and tool transformations are available after base and tool calibration, (3) can be rewritten as

$$\begin{aligned}\mathbf{T}_{\exp}^i&=\mathbf{T}_{base}^0\mathbf{T}_{base}^{err}(\mathbf{p}_{base},\boldsymbol{\varphi}_{base})\mathbf{T}_{robot}(\mathbf{q}^i,\Delta\mathbf{q})\times\\ &\times\mathbf{T}_{tool}^0\mathbf{T}_{tool}^{err}(\mathbf{p}_{tool},\boldsymbol{\varphi}_{tool})\end{aligned} \tag{5}$$

where $\mathbf{T}_{base}^0$ and $\mathbf{T}_{tool}^0$ are initial transformation matrices while after initial base and tool calibration, $\mathbf{T}_{base}^{err}(\mathbf{p}_{base},\boldsymbol{\varphi}_{base})$ expresses non-calibrated small errors $\mathbf{p}_{base},\boldsymbol{\varphi}_{base}$ in base transformation matrix estimation and $\mathbf{T}_{tool}^{err}$ in tool transformation matrix accordingly. Further we omit superscript "err" for base and tool error matrices and write simply $\mathbf{T}_{base}(\mathbf{p}_{base},\boldsymbol{\varphi}_{base})$, $\mathbf{T}_{tool}(\mathbf{p}_{tool},\boldsymbol{\varphi}_{tool})$. $\mathbf{T}_{\exp}^i$ corresponds to transformation matrix formed by experimental data $\mathbf{p}^i,\boldsymbol{\varphi}^i$. Let us define $\mathbf{T}_d^i=\left(\mathbf{T}_{base}^0\right)^{-1}\cdot\mathbf{T}_{\exp}^i$ and $\mathbf{T}_r^i(\mathbf{q}^i,\Delta\mathbf{q})=\mathbf{T}_{robot}(\mathbf{q}^i,\Delta\mathbf{q})\cdot\mathbf{T}_{tool}^0$. Then we can rewrite (5) as

$$\mathbf{T}_d^i=\mathbf{T}_{base}(\mathbf{p}_{base},\boldsymbol{\varphi}_{base})\cdot\mathbf{T}_r^i(\mathbf{q}^i,\Delta\mathbf{q})\cdot\mathbf{T}_{tool}(\mathbf{p}_{tool},\boldsymbol{\varphi}_{tool}) \tag{6}$$

Taking into account that homogenous transformation matrix T can be split into the rotational **R** and translational **p** components and presented as

$$T=\begin{bmatrix}\mathbf{R} & \mathbf{p}\\ 0 & 1\end{bmatrix} \tag{7}$$

The Cartesian coordinates $\mathbf{p}_i^d$ can be expressed in the following form

$$\mathbf{p}_d^i=\mathbf{p}_{base}+\mathbf{R}_{base}\mathbf{p}_r^i+\mathbf{R}_{base}\mathbf{R}_r^i\mathbf{p}_{tool} \tag{8}$$

In this step, assuming that errors in initial base location are small, the matrix $\mathbf{R}_{base}$ can be written as $\mathbf{R}_{base}=\left[\boldsymbol{\varphi}_{base}\times\right]+\mathbf{I}$, where $\mathbf{I}$ is 3×3 identity matrix and the operator $\left[\boldsymbol{\varphi}\times\right]$ transforms the vector $\boldsymbol{\varphi}=(\varphi_x,\varphi_y,\varphi_z)^T$ into the skew symmetric matrix. Then as shown in [10] (8) can be rewritten in matrix form as

$$\Delta\mathbf{p}^i=\mathbf{p}_d^i-\mathbf{p}_r^i=\left[\mathbf{I}\,|\left[\mathbf{p}_r^i\times\right]^T|\,\mathbf{R}_r^i\right]\begin{bmatrix}\mathbf{p}_{base}\\ \boldsymbol{\varphi}_{base}\\ \mathbf{u}_{tool}\end{bmatrix} \tag{9}$$

where $\mathbf{u}_{tool}=\mathbf{R}_{base}\mathbf{p}_{tool}$. Combining (11) for each i=1..m into one equation we get $\Delta\mathbf{p}=\mathbf{A}\cdot\left[\mathbf{p}_{base}\quad\boldsymbol{\varphi}_{base}\quad\mathbf{u}_{tool}\right]^T$, where $\Delta\mathbf{p}=\left[\Delta\mathbf{p}^1\quad...\quad\Delta\mathbf{p}^m\right]^T$ and

$$\mathbf{A}=\begin{bmatrix}\mathbf{I} & \left[\mathbf{p}_r^1\times\right]^T & \mathbf{R}_r^1\\ ... & ... & ...\\ \mathbf{I} & \left[\mathbf{p}_r^m\times\right]^T & \mathbf{R}_r^m\end{bmatrix} \tag{10}$$

Applying linear least-square technique to the above equation we get

$$\left[\mathbf{p}_{base} \quad \boldsymbol{\varphi}_{base} \quad \mathbf{u}_{tool}\right]^T = \left(\mathbf{A}^T\mathbf{A}\right)^{-1}\mathbf{A}^T\Delta\mathbf{p} \tag{11}$$

After that $\mathbf{p}_{tool}$ vector is found as $\mathbf{p}_{tool} = \mathbf{R}_{base}^T\mathbf{u}_{tool}$. To calculate tool orientation vector $\boldsymbol{\varphi}_{tool}$ let us consider (6) and its rotation part as

$$\mathbf{R}_d^i = \mathbf{R}_{base}\mathbf{R}_r^i\mathbf{R}_{tool} \tag{12}$$

Again we can transform equation to the form $\mathbf{B}\mathbf{R}_d = \mathbf{R}_r\mathbf{R}_{tool}$ with $\mathbf{R}_d = \left[\mathbf{R}_d^1 \ \ldots \ \mathbf{R}_d^m\right]^T$, $\mathbf{R}_r = \left[\mathbf{R}_r^1 \ \ldots \ \mathbf{R}_r^m\right]^T$, $\mathbf{B}=diag(\mathbf{R}_{base}^T \ldots \mathbf{R}_{base}^T)$ and similarly applying linear least-square technique

$$\mathbf{R}_{tool} = \left(\mathbf{R}_r^T\mathbf{R}_r\right)^{-1}\mathbf{R}_r^T\mathbf{B}\mathbf{R}_d \tag{13}$$

Vector $\boldsymbol{\varphi}_{tool} = (\varphi_x, \varphi_y, \varphi_z)^T$ is found from rotation matrix $\mathbf{R}_{tool}$. After $\mathbf{p}_{base}, \boldsymbol{\varphi}_{base}, \mathbf{p}_{tool}, \boldsymbol{\varphi}_{tool}$ are found we update initial estimation of $\mathbf{T}_{base}$ and $\mathbf{T}_{tool}$.

Step 2. On this step base and tool parameters are assumed to be known and the goal is to identify $\Delta\mathbf{q} = \left[\Delta q_1 \ldots \Delta q_6\right]^T$ vector. For this purpose, let us consider position part of (3) for *i*-th experimental point and define $\mathbf{p}_d^i$ as position part of $\left(\mathbf{T}_{base}\right)^{-1}\mathbf{T}_{\exp}^i$ and $\mathbf{p}_r^i$ as position part of $\mathbf{T}_{robot}(\mathbf{q}^i, \Delta\mathbf{q})\mathbf{T}_{tool}$. Eq. (3) can be linearized and written as

$$\Delta\mathbf{p}^i = \mathbf{p}_d^i - \mathbf{p}_r^i = \mathbf{J}^i(\mathbf{q}^i, \Delta\mathbf{q}, \mathbf{T}_{tool})\delta\mathbf{q} \tag{14}$$

where $\Delta\mathbf{p}$ is the residual vector corresponding to the *i*-th configuration, $\delta\mathbf{q}$ is the vector of joint offsets errors, $\mathbf{J}^i(\mathbf{q}^i, \Delta\mathbf{q}, \mathbf{T}_{tool})$ is Jacobian matrix computed for configuration $\mathbf{q}_i$ with given joint offsets and tool transformation matrix. Applying linear least-square method to find desired joint offsets error vector gives us

$$\delta\mathbf{q} = \left(\mathbf{J}^T\mathbf{J}\right)^{-1}\mathbf{J}^T\Delta\mathbf{p} \tag{15}$$

with $\mathbf{J} = [\mathbf{J}^1 \ldots \mathbf{J}^m]^T$, $\Delta\mathbf{p} = [\Delta\mathbf{p}^1 \ldots \Delta\mathbf{p}^m]^T$.

After that we update joint offset vector $\Delta\mathbf{q} = \Delta\mathbf{q} + \delta\mathbf{q}$ and repeat step 1. It should be noted, that parameters estimated on Step 1 and Step 2 are coupled and to get accurate values of joint off-setts it is required to repeat these steps iteratively. From our experience it is known that it is required to have only few iterations to ensure parameter estimate convergence.

IV. Experimental Results

The experiment setup is sown in Fig. 3. It contains humanoid AR-601M with fixed body with respect to the manipulator Kuka IIWA 14 R820 used for measurements. Fig. 1 shows in details anthropomorphic robot AR-601M which is in the focus of our study and kinematic scheme of its leg and hand. We are currently concentrated on stable gait algorithms [15]. Hence precise calibration of leg joints is essential for us. However, the calibration method we propose can be performed for humanoid's arms as well. Humanoid robot has 6 joints in each leg, with parameters L1=L2=0.28m

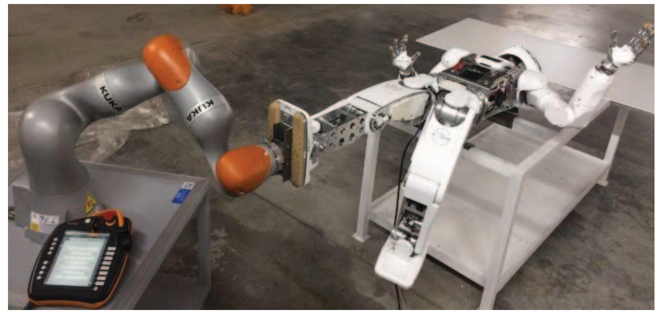

Figure 3. General view of experimental setup.

Before implementation on the real robot we carried out numerical simulations for the proposed algorithm. Firstly, we test it on the "ideal" experimental data, which was generated from robot's forward kinematics. In this case algorithm precisely finds joint offsets regardless of their value. Also in this case algorithm perfectly works even if we do not provide initial base and tool transformation matrices. Further we added normally distributed measurement noise to numerically generated experimental data. Variance of measurement noise was fixed from 0 to 1 mm to verify the algorithm robustness. Within this limit it was able to estimate correctly joint off-sets and tool/base parameters. Simulations show that precision of joint offsets calculation depends on number of experimental data and configurations.

One of the key issues in realization of the proposed algorithm with real humanoid robot using manipulator is that to achieve the best accuracy we need to choose leg configurations that are close to joint limits [16]. However, it is not always possible due to limited intersection of KUKA manipulator's and humanoid leg's workspaces. Therefore, we manually selected the upper and lower limit for each of the leg joint achievable for manipulator's end-effector and made measurements in that points. Totally we got 64 experimental points.

As a first step initial estimation of base frame location was done by rotating second and third joints. Rotating single joint gives us experimental points on a circle. Then circle center and circle normal vectors are located by fitting algorithm. Circle center defines frame center and circle normal vectors for second and third joints rotations define frame's x and y axes correspondingly. The third frame vector is found as cross product.

TABLE I. Base and Tool Frames Locations

	Base	Tool
x (m)	1.067	0.01
y (m)	0.634	-0.001
z (m)	0.344	-0.131
φ_x (rad)	2.178	-0.003
φ_y (rad)	-1.515	0.005
φ_z (rad)	1.963	-0.725

Further, using obtained measurement data, the two-step parameters identification algorithm proposed in previous Section has been applied. Fig. 4 shows that residual vector norm distribution before and after calibration. Notice that an average error has been reduced from 127 to approximately 4 mm.

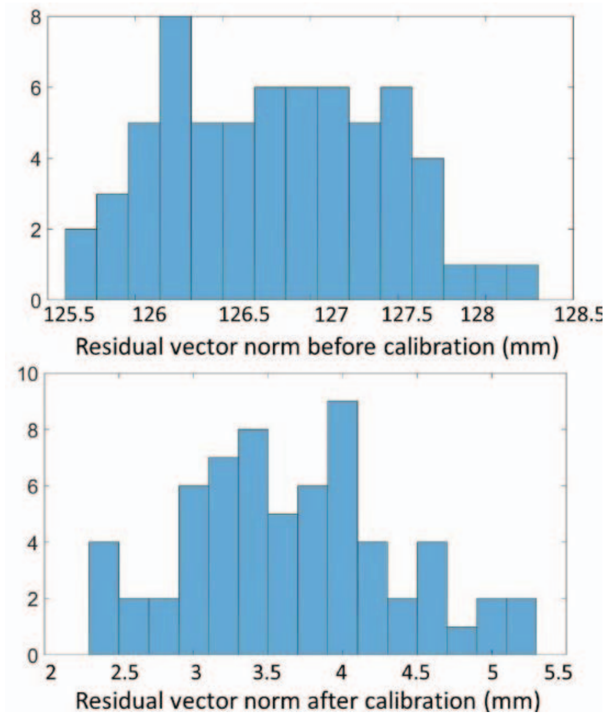

Figure 4. Histograms of residual values norm before calibration (upper) and after calibration (lower).

The estimates for base and tool parameters for carried out experiments are presented in Table I. Comparison of position values with direct estimates show a good agreement with identified one. Table II presents joint offsets values and estimates for their accuracy. As follows form experimental study, knee pitch and ankle pitch joints have the highest values of joint offsets, which directly affects on the motion capabilities of humanoid robot understudy.

TABLE II. JOINT OFFSETS

Joint	Δq_1	Δq_2	Δq_3
Offset (deg)	1±0.03	-0.2±0.07	-0.3±0.16
Joint	Δq_4	Δq_5	Δq_6
Offset (deg)	6.4±0.3	-8.4±0.34	-1.2±0.34

V. CONCLUSION

This paper presents humanoid robot joint calibration technique using KUKA LBR iiwa 14 R820 manipulator. Proposed algorithm uses position and orientation data measured by KUKA for different robot configurations and relies on least-square minimization of position and orientation residual vectors between kinematic model and experimental data. The calibration method is general and can be used for different robots. Experiments with real humanoid robot AR601M and its leg showed that it possible to find joint offsets with high accuracy. In future work the method will be extended to calculate elastostatic and dynamic parameters of the robots and particularly of humanoid limbs.

ACKNOWLEDGMENT

Part of the work was performed according to the Russian Government Program of Competitive Growth of Kazan Federal University.

REFERENCES

[1] F. Asano, H. Asoh, S. Kajita, "Online detection of calibration errors in humanoid robots", Signal and Information Processing Association Annual Summit and Conference (APSIPA), 2014 Asia-Pacific, 2014, pp. 1-6.

[2] A. Roncone, M. Hoffmann, U. Pattacini, G. Metta, "Automatic kinematic chain calibration using artificial skin: Self-touch in the iCub humanoid robot," 2014 IEEE International Conference on Robotics and Automation (ICRA), 2014, pp. 2305-2312.

[3] N. Guedelha, N. Kuppuswamy, S. Traversaro, F. Nori, "Self-calibration of joint offsets for humanoid robots using accelerometer measurements," 2016 IEEE-RAS 16th International Conference on Humanoid Robots (Humanoids), 2016, pp. 1233-1238.

[4] O. Birbach, B. Bäuml, U. Frese, "Automatic and self-contained calibration of a multi-sensorial humanoid's upper body," 2012 IEEE International Conference on Robotics and Automation, 2012, pp. 3103-3108.

[5] D. Maier, S. Wrobel, M. Bennewitz, "Whole-body self-calibration via graph-optimization and automatic configuration selection," 2015 IEEE International Conference on Robotics and Automation (ICRA), 2015, pp. 5662-5668.

[6] J.-H. Kim, J.-Y. Kim, J.-H. Oh, "Adjustment of Home Posture of Biped Humanoid Robot Using Sensory Feedback Control, Journal of Intelligent and Robotic Systems, 51 (2008) 421-438.

[7] T. Asfour, K. Welke, P. Azad, A. Ude, R. Dillmann, "The karlsruhe humanoid head," Humanoid Robots, 2008. Humanoids 2008. 8th IEEE-RAS International Conference on, IEEE, 2008, pp. 447-453.

[8] K. Yamane, "Practical kinematic and dynamic calibration methods for force-controlled humanoid robots," 2011 11th IEEE-RAS International Conference on Humanoid Robots, 2011, pp. 269-275.

[9] G. Du, P. Zhang, D. Li, "Online robot calibration based on hybrid sensors using Kalman Filters," Robotics and Computer-Integrated Manufacturing, 31 (2015) 91-100.

[10] A. Klimchik, Y. Wu, S. Caro, B. Furet, A. Pashkevich, "Geometric and elastostatic calibration of robotic manipulator using partial pose measurements," Advanced Robotics, 28 (2014) 1419-1429.

[11] B.W. Mooring, Z.S. Roth, M.R. Driels, "Fundamentals of manipulator calibration," Wiley New York, 1991.

[12] A. Nubiola, I.A. Bonev, "Absolute calibration of an ABB IRB 1600 robot using a laser tracker," Robotics and Computer-Integrated Manufacturing, 29 (2013) 236-245.

[13] J. Santolaria, J.-J. Aguilar, J.-A. Yagüe, J. Pastor, "Kinematic parameter estimation technique for calibration and repeatability improvement of articulated arm coordinate measuring machines," Precision Engineering, 32 (2008) 251-268.

[14] N. Maru, H. Kase, S. Yamada, A. Nishikawa, F. Miyazaki, "Manipulator control by using servoing with the stereo vision," Intelligent Robots and Systems' 93, IROS'93. Proceedings of the 1993 IEEE/RSJ International Conference on, IEEE, 1993, pp. 1866-1870.

[15] R. Khusainov, I. Shimchik, I. Afanasyev, E. Magid, "Toward a human-like locomotion: Modelling dynamically stable locomotion of an anthropomorphic robot in simulink environment," Informatics in Control, Automation and Robotics (ICINCO), 2015 12th International Conference on, 2015, pp. 141-148.

[16] J.-H. Borm, C.-H. Meng, "Determination of optimal measurement configurations for robot calibration based on observability measure," The International Journal of Robotics Research, 10 (1991) 51-63.